
EFDA–JET–CP(03)01-53

G. Saibene, P. J. Lomas, R. Sartori, P. Andrew, Y. Andrew, M. Becoulet,
G. D. Conway, K. Guenther, L. C. Ingesson, M. A. H. Kempenaars, A. Korotkov,
H. R. Koslowski, A. Loarte, J. S. Lonroth, D. McDonald, A. G. Meigs,
P. Monier Garbet, M. F. Nave, J. Ongena, V. V. Parail, C. P. Perez, F. G. Rimini,
S. Saarelma, S. Sharapov, J. Stober, P. R. Thomas
and JET EFDA Contributors

Pedestal and ELM Characterisation of Highly Shaped Single Null and Quasi Double Null Plasmas in JET

Pedestal and ELM Characterisation of Highly Shaped Single Null and Quasi Double Null Plasmas in JET

G. Saibene¹, P. J. Lomas², R. Sartori¹, P. Andrew², Y. Andrew², M. Becoulet³,
G. D. Conway⁴, K. Guenther², L. C. Ingesson^{1,5}, M. A. H. Kempenaars⁵,
A. Korotkov², H. R. Koslowski⁶, A. Loarte¹, J. S. Lonroth⁷, D. McDonald²,
A. G. Meigs², P. Monier Garbet³, M. F. Nave⁸, J. Ongena⁹, V. V. Parail²,
C. P. Perez⁶, F. G. Rimini³, S. Saarelma⁷, S. Sharapov², J. Stober⁴, P. R. Thomas³
and JET EFDA Contributors*

¹EFDA Close Support Unit (Garching), 2 Boltzmannstrasse, Garching, Germany

²Euratom/UKAEA Association, Culham Science Centre, Abingdon, OX14 3DB, UK

³Association Euratom-CEA, Cadarache, F-13108 St. Paul-lez-Durance, France

⁴Association Euratom-IPP, MPI für Plasmaphysik, 2 Boltzmannstrasse, Garching, Germany

⁵FOM Rijnhuizen, Associatie EURATOM-FOM, Nieuwegein, Netherlands

⁶Forschungszentrum Jülich GmbH, Institut für Plasmaphysik, EURATOM Association, Trilateral Euregio Cluster, 52425 Jülich, Germany

⁷Association EURATOM-Tekes, Helsinki Univ. of Techn., P.O. Box 2200, 02015 HUT, Finland

⁸Associação EURATOM/IST, Centro de Fusão Nuclear, 1049-001 Lisbon, Portugal

⁹ERM-KMS, Lab Plasma Physics, Brussels, Belgium.

*See Annex of J. Pamela et al., "Overview of Recent JET Results and Future Perspectives", Fusion Energy 2000 (Proc. 18th Int. Conf. Sorrento, 2000), IAEA, Vienna (2001).

Preprint of Paper to be submitted for publication in Proceedings of the
EPS Conference on Controlled Fusion and Plasma Physics,
(St. Petersburg, Russia, 7-11 July 2003)

“This document is intended for publication in the open literature. It is made available on the understanding that it may not be further circulated and extracts or references may not be published prior to publication of the original when applicable, or without the consent of the Publications Officer, EFDA, Culham Science Centre, Abingdon, Oxon, OX14 3DB, UK.”

“Enquiries about Copyright and reproduction should be addressed to the Publications Officer, EFDA, Culham Science Centre, Abingdon, Oxon, OX14 3DB, UK.”

ABSTRACT.

Simultaneous high confinement and density are routinely achieved in steady state conditions for $\sim 20\tau_E$ in JET with highly shaped plasmas. The normalised parameters required for the $Q=10$ inductive operation of ITER, namely $H_{98} \sim 1$, density $> 85\% n_{GR}$ and $\beta_N \sim 2$ with $q_{95} \sim 3$, are obtained in lower SN plasmas with $\delta_{sep} \sim 0.4 - 0.5$. These plasmas are characterised by an ETB with Type I ELMs. Above a certain pedestal density (typically $n_{ped} > 80n_{GR}$), the Type I ELM frequency decreases to few Hz, while the Type I ELM prompt energy losses do not increase or even decrease [1] compared to those at a lower density, and H_{98} does not decrease any longer with density. The change in fELM corresponds to enhanced energy and particle losses between ELMs, attributed to the presence of an additional edge relaxation mechanism, identified, by analogy with other experiments [2, 3, 4], as type II ELMs. Steady state Type II ELMs regime has been obtained in AUG [2], for plasma configuration near to double null (QDN), high pedestal density and $q_{95} > 4$ for $\beta_p \sim 1$. The possible requirement of QDN plasma geometry to achieve Type I ELM suppression is of some concern for the extrapolation of this regime to ITER, since ITER is not designed to accommodate high particle fluxes or power fluxes to the top x-point region.

1. THE EXPERIMENT.

This paper presents the results of experiments carried out in JET to study the plasma pedestal and ELM behaviour of high density/high confinement ELMy H-modes, focusing on the exploration of the effects of the plasma boundary magnetic geometry (triangularity δ , as well as proximity to Double Null DN) and of q_{95} on the pedestal parameters, edge stability and ELM losses. These experiments were aimed at the study of Type I ELMs at high density and of the access to steady state Type II ELM regime for JET plasma conditions, comparing pedestal and ELM characteristics in high δ SN and QDN plasmas, in similar experimental conditions. The main characteristics of the plasma configurations and general parameters used in this study are summarised in table 1. The experiments were carried out mainly in the HT3 configuration (see also [5]) and in QDN. The additional heating was mainly by NB injection (13–16MW), with the addition of 2-3MW of central ICRH (H minority heating). In QDN, machine safety considerations (in particular issues of plasma vertical stability to large type I ELMs in high elongation plasmas) restricted the operations to high density, where the Type I ELM size is reduced, and fast vertical excursions of the plasma more easily controlled.

2. GENERAL RESULTS, CONFINEMENT AND PEDESTAL PARAMETERS.

At 2.5MA and $q_{95} \sim 3$ to 3.6, the plasma edge enters the mixed type I-II ELM regime for both SN and QDN configurations, for $n_{ped} \sim 80\% n_{GR}$, with typical Type I ELM frequency of 6 to 10Hz. The lower f_{ELM} is measured for the QDN plasmas, for otherwise similar plasma conditions. The reduction of δ_{sep} in steps from 2cm to quasi pure double null geometry does not result in the suppression of Type I ELMs. Notably, the approach to QDN reduces by up to a factor of ~ 2 the amount of external fuelling required to reach a certain steady state n_{ped} compared to the HT3 plasmas, consistent with increased particle recycling from the upper x-point region and, possibly, higher neutral penetration. The

confinement enhancement factor H98 for SN (HT3) at 2.5MA/2.7T and that of QDN at same I_p/B_t are compared in figure 1. Each point represents a plasma discharge and the shaded areas indicate discharges in the mixed Type I-II regime. The normalised confinement of the QDN plasmas is 10 to 20% lower than the reference HT3, for the same I_p and normalise n_{ped} . The lowest H98 values in QDN shape correspond to plasmas with the lowest δ_{sep} , i.e. closest to pure double null. For both configurations, the core density profiles are weakly peaked ($n_{core}/n_{ped} \sim 1.2$), and the QDN reach higher absolute densities. The positive density dependence of H98 ($H98 \propto n^{0.4}$) does not entirely account for the reduced normalised confinement. Experimentally, high edge safety factor ($q_{95} \sim 4$ or larger) facilitate the access to steady state Type II/Grassy ELM regimes in ASDEX-U [2] and JT-60U [3]. This was tested in the JET experiments, where q_{95} was increased in both SN and QDN configuration, and a gas scan and proximity to double null scan carried out. In the case of the SN, q_{95} was increased to 4.6 at constant I_p (experiments where q_{95} was increased at constant B_t for SN are reported in [2]), while for QDN q_{95} was raised from 3.1 to 3.6 and then to 4.1 by decreasing I_p . Increasing q_{95} , for both SN and QDN results in a strong increase of the ELM frequency (by factor of 2 to 3) and, as shown in figure 1, reduces the normalised confinement. Moreover, the maximum pedestal (and core) density achievable before the type I-III ELM transition is substantially reduced compared to the lower q_{95} cases, from $\sim 90\%$ down to 60-70% of n_{GR} . The analysis of the pedestal parameters (shown in fig.2) is consistent with the picture given by the confinement. The high confinement at high density obtained in the SN/ $q_{95} = 3.6$ corresponds to a clamping of the T_{ped} for increasing density, i.e. to an effective increase of the pedestal pressure with density (see also [5]) and to the onset of mixed Type I-II ELMs. This is the case also for the QDN at low q_{95} , although T_{ped} is reduced compared to the SN plasmas, as is H98. Increasing the q in SN results in a reduction of the pedestal pressure as well as in an early transition to type III ELMs (figures 1 and 2, open symbols), lower pedestal parameters and confinement. The access to Type II ELMs may occur at lower n_{ped} in SN at higher q_{95} (see section 4) but this change in ELM regime does not result in improved pedestal or core performance. QDN plasmas at high q_{95} show a similar behaviour to the SN discharges. The access to mixed type I-II ELM regime is essentially precluded in these conditions, with the transition to Type III ELMs taking place at low n_{ped} .

3. TYPE II ELMs CHARACTERISATION.

An interpretation of the change of Type I ELM behaviour at high density and increased inter-ELM losses comes from the analysis of magnetic (and density) fluctuations. Type II ELMs in JET are accompanied by an increase of the intensity of broadband magnetic fluctuations at low frequency, associated with the changes in the pedestal and ELM behaviour described above [4]. These broadband MHD events have been identified as washboard modes [6, 7], and the increase of the intensity of these modes (always observed in the edge of Type I ELM My H-modes in JET) is associated with increased energy and particle losses between Type I ELMs [7, 8]. Figure 3 compares the MHD fluctuation for four representative discharges in this study: two SN at $q_{95} = 3.6$ with type I and mixed Type I-II ELMs, a SN versus a QDN, at the same I_p and B_t , both with mixed Type I-II ELMs, and last low q_{95}

versus high q_{95} in SN. The first plot of figure 3 illustrate the typical change in the MHD activity between Type I ELMs, at low and high pedestal density. The intensity of the MHD activity decreases at high frequency (>40 kHz), while is enhanced around the 20kHz level (± 10 kHz). This is clearly visible in the spectrogrammes for the two discharges (figure 4, plots 1 and 2), which also show the reduction in the type I ELM frequency in the presence of the enhanced inter-ELM MHD activity. The second plot in figure 3 shows that the washboard mode signature for mixed Type I-II ELMs in SN and QDN is quite similar, with the intensity of fluctuations having the same frequency distribution for both configurations (see also figure 4, plot 3). Also in figure 3, plot 3 compares the washboard mode intensity for two SN discharges at different q_{95} . Although the reduction of the high frequency MHD component is similar for the two cases, at high q_{95} the characteristic intensity enhancement in the 20 kHz range is absent or strongly reduced compared to the low q_{95} cases. The interpretation of such a behaviour is for the moment pending, but it is obvious that increasing the edge q does not seem to facilitate the access to the mixed Type I-II regime in JET, and even less open up access to total Type I ELM suppression. The results for the QDN at $q_{95} = 4.1$ are similar, and no clear Type II ELM phases have been observed, for the investigated fuelling rates and Δ_{sep} .

Previous analysis of mixed Type I-II ELMy H-mode plasmas [4] had shown that the presence of enhanced MHD activity between ELMs corresponds to a clamping of the pedestal temperature. In fact, after the Figure 5: density fluctuation measurement in SN, type I (left), and mixed Type I-II (right). Same discharges as for figure 4, plots 1 and 2. Fast (100 kHz) interferometry measurements in the region of the top of the pedestal show that the increased broadband MHD activity does also correspond to a similar increase in the density fluctuations, as illustrated in figure 5 for the same SN 2.5MA/2.7T discharges of figure 4, linking the increase of the washboard mode intensity not only to a saturation of T_{ped} , but also to increased particle losses between Type I ELMs (see also [7, 8]). Since the interferometer chord used for these measurements is vertical and going across the approximate position of the pedestal top, this could indicate that the MHD modes are localised around the pedestal top region, at least at high n_{ped} . An indirect confirmation of this finding comes from the analysis of the density fluctuations measured with a heterodyne reflectometer, with maximum cut-off density of $5.1 \times 10^{19} \text{ m}^{-3}$. The density profiles are from pulses 59344, a repeat of the SN Type I ELM discharge 57897, and 59345, a repeat of the SN mixed Type I-II discharge 57987, both discussed in detail earlier. The position of the cut-off layer in the pedestal gradient region for both sets of pulses is shown in fig.6. A lower cut-off density was selected for pulses 59344/57897 (fig.6), to compare the density fluctuation levels in similar relative positions in the gradient region. The corresponding intensity of the density fluctuations is shown in fig.7. No significant difference in the frequency distribution of the fluctuations in the steep gradient region of the pedestal is observed, between pure Type I and mixed Type I-II ELMs (both for SN and QDN). In particular no enhanced broadband fluctuations are observed ~ 20 kHz, in contrast to interferometry data, suggesting a very narrow region of edge-enhanced particle transport, possibly localised near the pedestal top. The decrease in the absolute intensity may be related to changes of \sqrt{n} , and is not related to changes in turbulence.

4. TYPE II ELM LOSSES.

The analysis of the rate of rise of the stored energy between type I ELMs shows that dW/dt is not a constant, even for constant average plasma conditions, with dW/dt varying from ELM to ELM, as well as in time, between two ELMs. For the high δ plasmas analysed in this paper, dW/dt varies from ~ 10 to $\sim 0\text{MJ s}^{-1}$. A qualitative correlation between dW/dt and the intensity of washboard modes amplitude is found, in a similar way as for T_{ped} between ELMs [7]. In spite of the ELM-to-ELM variation of dW/dt , one finds that the continuous losses in the Type II ELMs phases reduce the power carried by Type I ELMs, PELM, by more than a factor of 2 [4, 5]. In the case of the 2.5MA/2.7T plasmas, P_{ELM} is reduced from 50-60% down to 27% in SN plasmas and to 21% for QDN. Nonetheless, the pedestal pressure is still evolving in the Type II phases, indicating that these additional losses are not sufficient to suppress Type I ELMs completely. In particular, the edge particle refuelling rate in Type II ELM phases is reduced by a ~ 2 compared to pure Type I ELM plasmas (fig.8), but dn/dt is still >0 . Figure 8 also shows that the particle refuelling rate increases with q_{95} , with dn/dt at high q_{95} being a factor 1.4 to 1.8 higher than at lower q_{95} , for similar external gas fuelling. This, not surprisingly, results in a correlation between the higher refuelling rate and type I ELM frequency (fig.9), although the reason why high q_{95} should result in a better effective particle confinement in the edge is not, to date, understood. This change in edge particle transport and the consequent increase of fELM may partially explain the reduced access to type II ELMs at high q_{95} in JET.

5. ASDEX SIMILARITY EXPERIMENT.

The role of the plasma geometry in Type I ELM suppression was also investigated in JET by carrying out a similarity experiment with ASDEX-Upgrade (see table 1, QDN2). In this configuration, with $\sim 3\text{MW}$ of NB power and no external gas fuelling, long ELM free phases, up to 1.8s, were obtained, with constant W and $H_{98} \sim 1$ for $\sim 6\tau_E$. Although no ELMs are observed in this period, both n_{ped} and $T_{i,\text{ped}}$ are constant, with $n_{\text{ped}} \sim 2.2 \times 10^{19} \text{ m}^{-3}$ and $T_{\text{ped}} \sim 370\text{eV}$, corresponding to a local $v^* \sim 0.9$, in line with expectations. Broadband MHD fluctuations in the 20-30kHz range are present during the ELM-free phase, but incomplete data do not allow the determination of the mode numbers for mode identification and comparison with other JET data. The plasmas core is evolving throughout the ELM-free phase, with continuous density peaking and increasing radiation, leading to sawtooth suppression and termination of the H-mode by core radiative collapse. Experiments are planned to better document these results, attempt to combine ELM suppression with steady state core conditions and study the possible extension of this regime to higher I_p/B_t .

SUMMARY AND CONCLUSION.

To date, complete Type I ELM suppression has not been achieved in JET in steady state conditions, although at high shaping and density mixed phases of Type I and Type II ELMs are observed, both for SN and QDN plasmas. Long periods of Type II ELMs (up to 150ms in QDN) are obtained at high n_{ped} , associated with an increase of magnetic and density fluctuations, compared to levels in pure

Type I ELMy H-modes. The location of these enhanced fluctuation region is likely to be near the pedestal top. Increasing q_{95} from ~ 3 to ~ 4.5 (by varying either I_p or B_t), does not facilitate the access to the Type II ELM regime, in contrast to indications from other experiments. In general, at high q_{95} , the Type I ELMs frequency is much higher than at $q_{95} \sim 3$ (typical for JET ELMy H-modes), the plasma global confinement is reduced, the Type II activity weakens, with the Type I-III transition occurring at lower pedestal density than at lower q_{95} . The enhanced ~ 20 kHz magnetic fluctuations with Type II ELMs are identified with strong washboard modes, possible responsible for the increased inter-ELM transport. Power balance calculations do indeed show that the power carried by ELMs is reduced by more than a factor of two in the presence of enhanced MHD between ELMs, with PELM going from 50-60% down to 27% in SN plasmas and to 21% for QDN. Evaluation of the inter-ELM refuelling rate shows that enhanced particle losses associated to type II ELMs are not sufficient to drive the pedestal to steady state. Control of the density rise rate at the plasma edge is crucial for achieving steady state Type II ELMs at high confinement, in particular for plasmas near to DN (T_{ped} saturates between ELMs). In JET (and ITER), the long absolute particle confinement time may require active control of recycling in the upper x-point region as well as of fluxes from the main chamber/limiters.

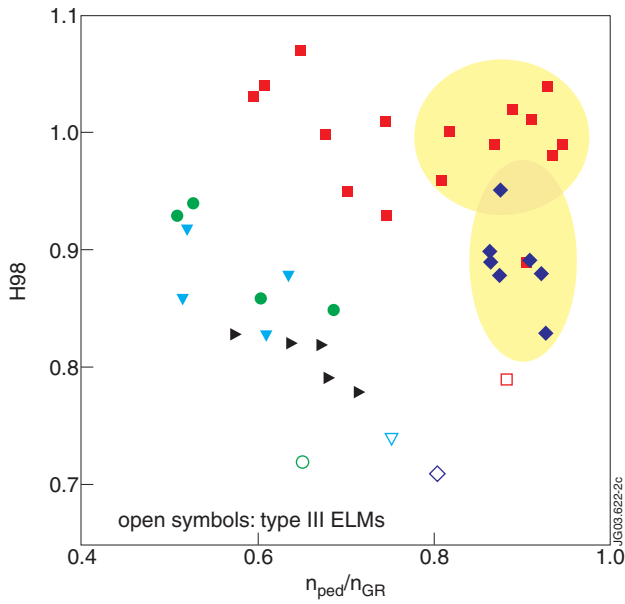
REFERENCES

- [1]. A. Loarte et al., PPCF **44** (2002) 1815
- [2]. J. Stober et al., Nucl Fus **41** (2001) 1123
- [3]. Y. Kamada and JT-60 Team, Nucl Fus **41** (2001) 1311
- [4]. G. Saibene et al., PPCF **44** (2002), 1769
- [5]. R. Sartori et al., this conference, paper P-1.101
- [6]. P. Smeulders et al., PPCF **41** (1999), 1303
- [7]. C. P. Perez et al., submitted to PPCF
- [8]. R. Koslowski et al., this conference, paper P-1.102

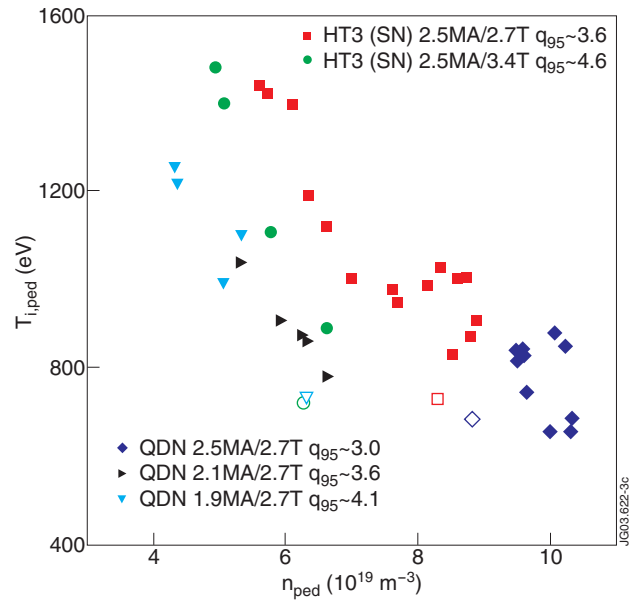
Null	Name	I_p (MA)	B_t (T)	q_{95}	κ_{sep}	$\delta_{sep, average}$
SN	ITER-like	2.5	2.7	3.1	1.77	0.46
SN	HT3	2.5	2.7-3.4	3.6-4.6	1.74	0.42
QDN	QDN (Δ_{sep} from >21 to <1cm)*	2.5-2.1-1.9	2.7	3-3.7-4.1	1.75 to 1.9*	0.43 to 0.5*
QDN2	Asdex similarity	0.8				

JG03.622-1c

Table 1: summary of geometry and main parameters of the plasma discharges analysed in this paper.



JG03.622-2c



JG03.622-3c

Figure 1: H_{98} versus n_{ped} normalised to n_{GR} . Same legend as fig.2.

Figure 2: Pedestal ion temperature versus density for the same plasmas of fig.1.

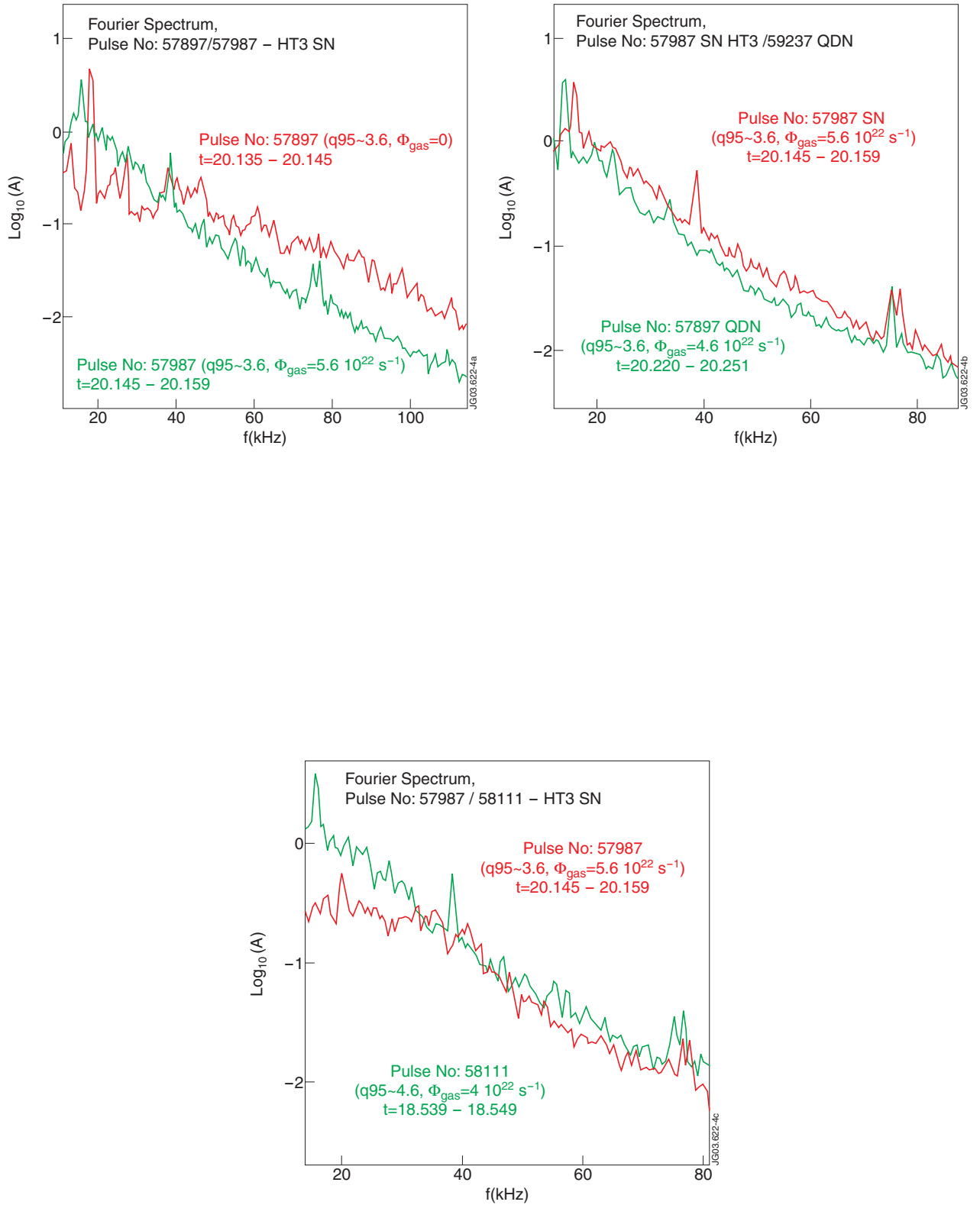


Figure 3: Comparison of the intensity of the washboard mode for 3 pairs of pulses: 1. HT3 at low q Type I (red) and Type II (green), 2. SN versus QDN at 2.5MA/2.7T, Type II phases, and last to the right, HT3 at low and high q_{95} . The low q pulse in plot 3 has mixed Type I-II ELMs. Note that the high frequency part of the spectrum is similar for both q_{95} , but the high q_{95} lacks the enhanced MHD at low frequency, typical of Type II ELM phases.

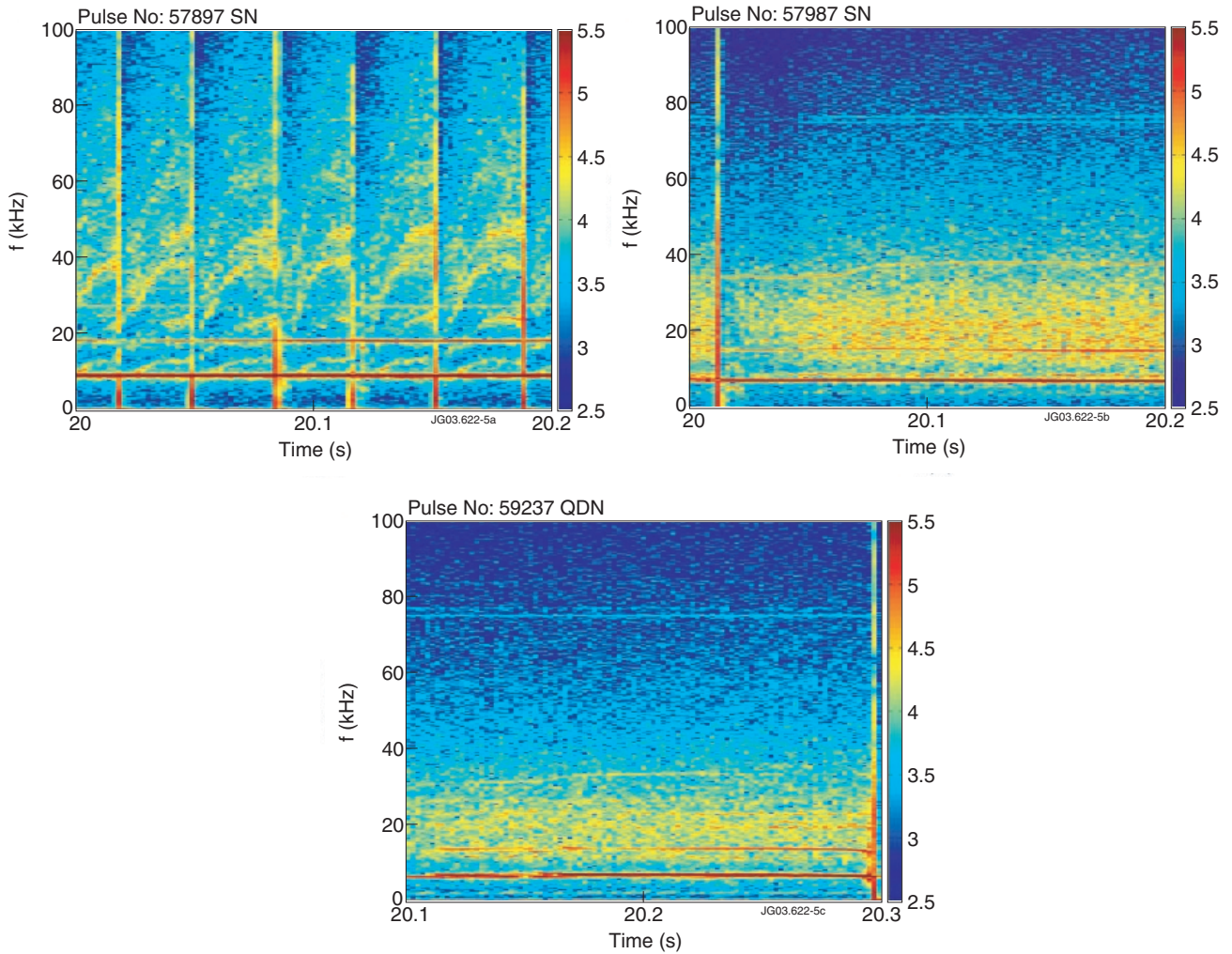


Figure 4: Spectrogrammes for 3 of the plasma discharges described above: SN HT3 2.5MA/2.7T Type I; in the middle HT3 2.5MA/2.7T with Type II ELMs, and last QDN at 2.5MA/2.7T with Type II ELMs. The intense and narrow vertical bands are type I ELMs, the horizontal continuous modes are correlated to sawtooth activity.

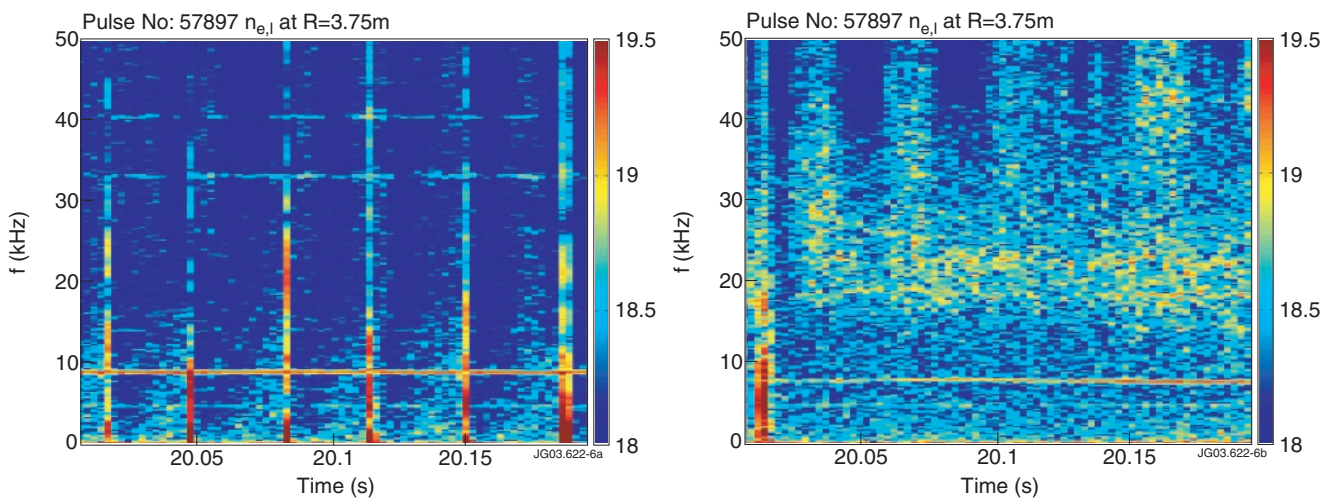


Figure 5: Density fluctuation measurement in SN, type I (left), and mixed Type I-II (right). Same discharges as for figure 4, plots 1 and 2.

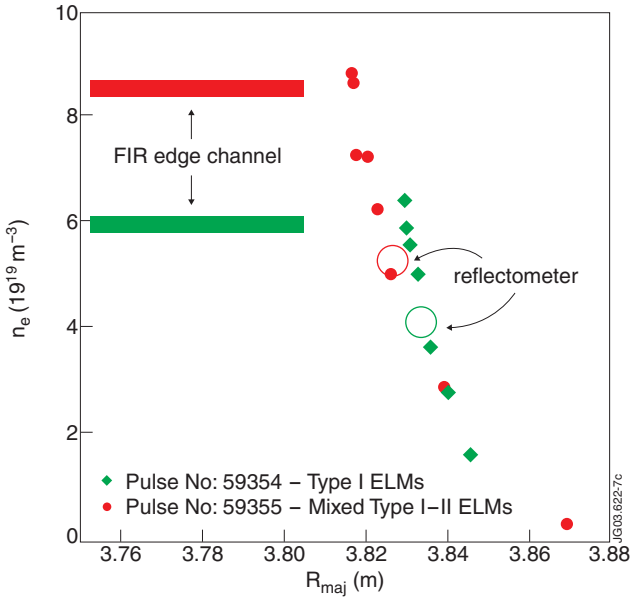


Figure 6: Position of the cut-off density layer in the pedestal gradient region for Pulse No's: 59354 and 57897 (SN, Type I) and 59355/57987 (SN, mixed Type I-II).

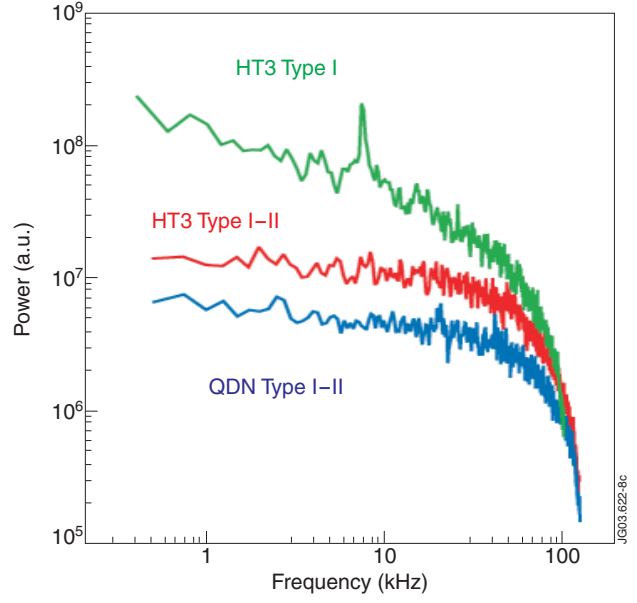


Figure 7: Intensity of the density fluctuations for Pulse No's: 57897 (green), 57987 (red), and for comparison, the QDN 2.5MA/2.7T, 59237 (blue)

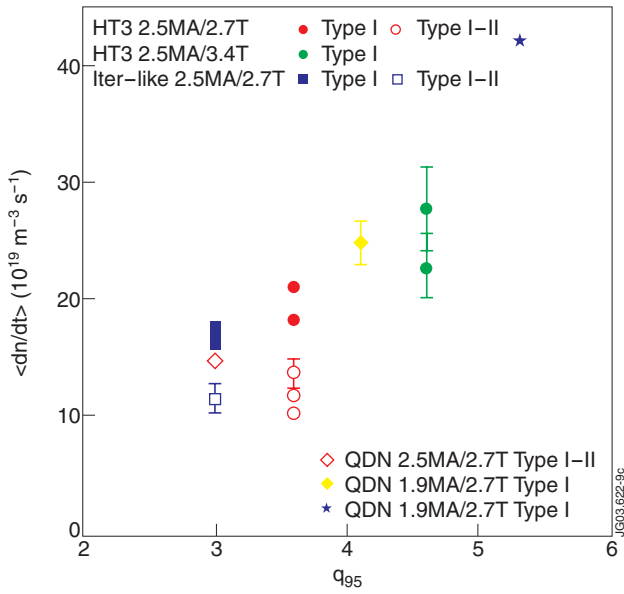


Figure 8: Comparison of the particle re-fuelling rate between Type I ELMs for various plasma conditions.

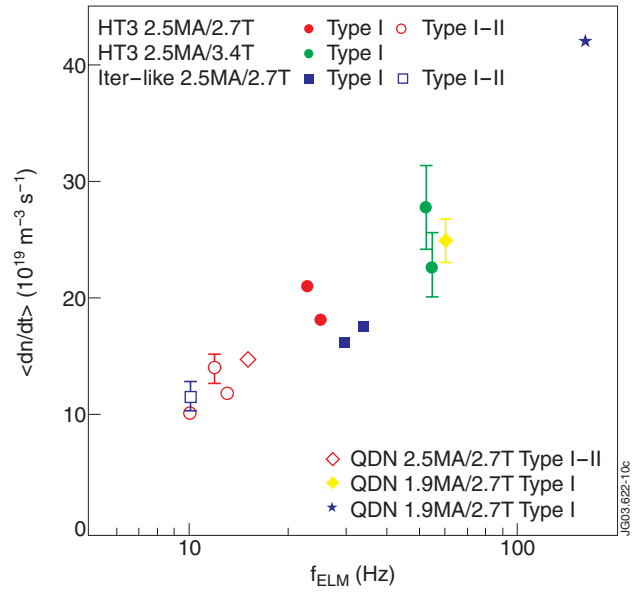


Figure 9: Particle re-fuelling rate versus Type I ELM frequency, for the same set of data as figure 8.